



## Article

# Tomato (*Solanum lycopersicum* L.) YTH Domain-Containing RNA-Binding Protein (YTP) Family Members Participate in Low-Temperature Treatment and Waterlogging Stress Responses

Yidan Zhang <sup>1</sup>, Tianli Guo <sup>2</sup>, Jingyuan Li <sup>1</sup>, Libo Jiang <sup>1</sup> and Na Wang <sup>1,\*</sup>

- <sup>1</sup> College of Life Sciences and Medicine, Shandong University of Technology, Zibo 255000, China; 22120702031@stumail.sdut.edu.cn (Y.Z.); 21120702071@stumail.sdut.edu.cn (J.L.); libojiang@sdut.edu.cn (L.J.)
- <sup>2</sup> State Key Laboratory of Crop Stress Biology for Arid Areas, College of Horticulture, Northwest A&F University, Xianyang 712100, China; guotl@gxu.edu.cn
- \* Correspondence: wang1993na@sdut.edu.cn; Tel./Fax: +86-533-2781329

**Abstract:** YT521-B homology (YTH) domain-containing RNA-binding proteins (YTPs) are important N<sup>6</sup>-methyladenosine (m<sup>6</sup>A) readers that have crucial roles in determining the destiny of m<sup>6</sup>A-modified RNAs, which are the most widespread RNA modifications in eukaryotes. Tomatoes (*Solanum lycopersicum* L.) hold significant importance in both dietary consumption patterns and scientific inquiries. While the YTP gene family has been characterized in tomatoes, their specific reactions to the low temperature and waterlogging stresses remain to be elucidated. In our study, nine tomato *SIYTPs* could be divided into five subclasses, YTHDFa-c and YTHDCa-b. After gene cloning and measuring their expression levels under stress conditions, it was revealed that *SIYTP8* exhibited increased sensitivity to low-temperature treatment, while the expression levels of *SIYTP9* were notably upregulated in leaf tissues subjected to waterlogging conditions. As members of the YTHDFc subfamily, *SIYTP8* and *SIYTP9* are both localized in the cytoplasm. Nevertheless, overexpression (OE) of *SIYTP8* increased the sensitivity of tomato plants to low-temperature treatment, which was manifested by a higher accumulation of malondialdehyde (MDA) and hydrogen peroxide (H<sub>2</sub>O<sub>2</sub>) and a weaker reactive oxygen species scavenging ability compared to wild-type (WT) tomatoes. However, in comparison to WT plants, the leaves of *SIYTP9* OE tomatoes showed higher chlorophyll content and a stronger reactive oxygen species scavenging ability after 3 days of waterlogging treatment, thereby increasing the resistance of tomatoes to waterlogging stress. Moreover, in order to investigate the possible molecular mechanisms underlying their responses to the low temperature and waterlogging stresses, the transcription factors and interacting protein networks associated with *SIYTP8/9* promoters and proteins were also predicted, respectively. These results could fill the gap in the understanding of tomato YTPs in response to the low temperature and waterlogging stresses, while also providing a theoretical and experimental basis for subsequent studies on their molecular mechanisms.

**Keywords:** tomato; m<sup>6</sup>A; YT521-B homology (YTH); low temperature; waterlogging



**Citation:** Zhang, Y.; Guo, T.; Li, J.; Jiang, L.; Wang, N. Tomato (*Solanum lycopersicum* L.) YTH Domain-Containing RNA-Binding Protein (YTP) Family Members Participate in Low-Temperature Treatment and Waterlogging Stress Responses. *Horticulturae* **2024**, *10*, 522. <https://doi.org/10.3390/horticulturae10050522>

Academic Editor: Xiaohu Zhao

Received: 18 April 2024

Revised: 9 May 2024

Accepted: 14 May 2024

Published: 17 May 2024



**Copyright:** © 2024 by the authors. Licensee MDPI, Basel, Switzerland. This article is an open access article distributed under the terms and conditions of the Creative Commons Attribution (CC BY) license (<https://creativecommons.org/licenses/by/4.0/>).

## 1. Introduction

There are more than 170 kinds of modifications on RNA molecules, such as N<sup>6</sup>-methyladenosine (m<sup>6</sup>A), N<sup>1</sup>-methyladenosine (m<sup>1</sup>A), and N<sup>4</sup>-acetylcytidine (ac<sup>4</sup>C) [1]. Among them, the functions of the m<sup>6</sup>A modification are better documented than other modifications. Nonetheless, the m<sup>6</sup>A modification is the most common and widespread post-transcriptional modification in eukaryotic RNAs [2]. The functional role of the RNA m<sup>6</sup>A modification relies on the involvement of its writers (m<sup>6</sup>A methyltransferases), readers (proteins responsible for m<sup>6</sup>A binding and recognition), and erasers (m<sup>6</sup>A demethylases) [3].

Writers and erasers determine the presence and dynamics of m<sup>6</sup>A, leading to differential levels of the RNA m<sup>6</sup>A modification across different growth stages and in response to varying environmental conditions [4]. The precise regulation of m<sup>6</sup>A on RNA metabolism is also dependent on both direct and indirect recognition by proteins known as m<sup>6</sup>A readers. YTH domain-containing RNA-binding proteins (YTPs) represent a class of RNA m<sup>6</sup>A readers, with their YTH domain being identified as directly interacting with the m<sup>6</sup>A molecule through an ‘aromatic pocket’. In this structural arrangement, two or three tryptophan residues effectively encase the m<sup>6</sup>A site [5]. The YTH domain, consisting of approximately 150 amino acids, exhibits a high degree of conservation among diverse eukaryotic organisms, including mammals (humans), fungi (yeast), and plants [5].

In humans and other mammals, there are five YTPs that can bind with the m<sup>6</sup>A modification in RNAs. These YTPs can be divided into five subclasses, i.e., YTHDFa-c (YTH domain-containing family protein a-c) and YTHDCa-b (YTH domain-containing protein a-b) [6–11]. Subcellular localization varies among members of different subclasses. YTHDF proteins (DFa, DFb, and DFc) are located in the cytoplasm and consist of a C-terminal YTH domain along with a substantial low-complexity region. Studies have demonstrated that YTHDFs have the capacity to interact with all m<sup>6</sup>A sites present in mRNA. YTHDCa is predominantly localized in the nucleus and features a central YTH domain in conjunction with several other functional domains. Conversely, YTHDCb is a nucleocytoplasmic protein that includes a C-terminal YTH domain as well as a DEAD-box RNA helicase domain. YTHDCa is known to interact with specific m<sup>6</sup>A sites within mRNAs and noncoding RNAs, while YTHDCb predominantly interacts with m<sup>6</sup>A-modified noncoding RNAs [12].

Plant genomes are characterized by a higher abundance of YTPs in comparison to other eukaryotes, with *Arabidopsis* containing 13 YTPs (*Arabidopsis thaliana*) [13], rice having 12 YTPs (*Oryza sativa*) [14], tomatoes possessing 9 YTPs (*Solanum lycopersicum*) [15], and wheat exhibiting 39 YTPs (*Triticum aestivum*) [16]. Among the 13 *Arabidopsis* YTPs, ECT2 (AT3G13460.1; EVOLUTIONARILY CONSERVED C-TERMINAL REGION 2, which was named before the identification of the YTH domain in plants) was initially identified as an m<sup>6</sup>A reader and has been demonstrated to interact with ECT3 (AT5G61020.1) and ECT4 (AT1G55500.5) in the cytoplasm. This interaction enhances the m<sup>6</sup>A-binding affinity and demonstrates genetic redundancy in *Arabidopsis* [17]. In accordance with their spatial proximity, ECT3 demonstrates a significant overlap in target genes with ECT2. Moreover, the collective action of ECT2, ECT3, and ECT4 serves to stabilize the m<sup>6</sup>A-modified mRNAs they target. However, it is noteworthy that this stabilization process does not exert an influence on the translation process, thereby indicating a post-transcriptional regulatory role of these proteins in modulating mRNA abundance [18,19]. A recent investigation revealed that ECT1 (AT3G03950.3) undergoes liquid–liquid phase separation (LLPS) to generate cytosolic biomolecular condensates, namely processing bodies and stress granules, in response to salicylic acid (SA) or bacterial pathogens. This process enables the sequestration of SA-induced m<sup>6</sup>A modification-prone mRNAs by ECT1 within these condensates, subsequently promoting their degradation [20]. In addition to the model plant *Arabidopsis*, analogous proteins have been identified in other plant species, exemplified by MhYTP2 in apple, as documented by Guo et al. [21]. Similarly, in tomatoes, the genes *SlYTH1* and *SlYTH2*, encoding hypothetical RNA m<sup>6</sup>A readers, have been found to exert discernible impacts on plant growth and fruit morphology [22,23]. These findings shed light on the conservation and functional significance of m<sup>6</sup>A-associated proteins across diverse plant taxa, which play crucial roles in plant development as well as in responses to both biotic and abiotic stresses.

Tomato (*Solanum lycopersicum* L.) is one of the most widely cultivated vegetables globally, which is also a frequently used model plant used in scientific research. Low temperature and waterlogging stress severely affect the quality and yield of tomatoes. To our knowledge, the functions of tomato YTP family members in low temperatures and waterlogging stress responses have not been thoroughly analyzed. Thus, the aim of this

study was to explore the key *SIYTP* gene family members participating in chilling and waterlogging stress responses. After the identification of *SIYTP* gene family members in the tomato genome, gene cloning and qRT-PCR will be conducted to measure their expression patterns under these stress conditions. Subcellular localization experiments can reveal the cellular compartments where the key *SIYTP* members exert their biological functions. Through the genetic transformation of tomatoes, transgenic plants could be obtained to verify the effect of *SIYTP* expressions on tomato resistance. These results could fill the gap in the understanding of tomato YTPs in response to low temperatures and waterlogging stress, while also providing a theoretical and experimental basis for subsequent studies on the molecular mechanisms and assistance of tomato resistance breeding.

## 2. Materials and Methods

### 2.1. Identification and Analysis of the *SIYTP* Gene Family

The sequences of the 13 identified AtYTPs were acquired from the Arabidopsis genome database TAIR (<https://www.arabidopsis.org/>, accessed on 13 May 2024), while those of the tomato genome were obtained from the Sol Genomics Network (<https://solgenomics.net/>, accessed on 13 May 2024). Then, *SIYTP*s were detected through two iterations of BLASTP analysis conducted using TBtools [24]. Following this, the ExpASY was utilized to calculate the coding sequence (CDS) length, isoelectric point (pI), and molecular weights (MWs) of all the forecasted *SIYTP*s [25]. The chromosomal coordinates for the *SIYTP* genes were extracted from the GFF3 reference file of the tomato genome. Utilizing TBtools software (v2.096) in conjunction with the tomato genomic annotation GFF3 file, the positional mapping of *SIYTP* genes onto chromosomes was performed [24]. Gene numbers per 300 kb of chromosomes are shown on each chromosome with different colors.

A neighbor-joining (NJ) phylogenetic tree was generated for the full-length sequences of AtYTPs and *SIYTP*s using MEGA7.0 with 1000 bootstrap replicates. Additionally, a multiple sequence alignment of all *SIYTP*s was conducted using MEGA7.0. Moreover, NCBI Batch CD-Search and TBtools were utilized to analyze and visualize the gene structures and conserved domains [24,26]. To identify conserved motifs in the genes, the MEME program (<https://meme-suite.org/meme/>, accessed on 13 May 2024) was employed with specific parameters. The optimum motif width was set between 15 and 50, while the number of repetitions was either zero or one. Additionally, a maximum number of 10 motifs was identified [27].

Prediction of promoter cis-acting elements was carried out using PlantCARE [28]. To gain an insight into the potential function of *SIYTP*s under various stress responses, we reviewed the available expression data obtained from tomato microarray chip experiments (<https://geneinvestigator.com/>, accessed on 13 May 2024). Expression data were collected from and visualized via the Geneinvestigator website [29].

### 2.2. Plant Growth and Treatments

Seeds of Micro-Tom (*S. lycopersicum* cv. Micro-Tom) were obtained from State Key Laboratory of Crop Stress Biology for Arid Areas/Shaanxi Key Laboratory of Apple, College of Horticulture, Northwest A&F University (Yangling, Shaanxi, China). Micro-Tom seedlings were cultivated in the walk-in plant growth chamber at the Horticultural college of Northwest A&F University (34°20' N, 108°24' E). Seedlings were grown in plastic pots (7 × 7 cm) filled with soil/perlite/vermiculite (4:1:1, v:v:v). Light intensity was set to 660 μmol m<sup>-2</sup> s<sup>-1</sup> and characterized by a 16 h day and 8 h night cycle, with a day/night temperature regimen of 25 °C/20 °C. Roots, stems, and leaves were harvested from 30-day-old seedlings for quantitative real time polymerase chain reaction (qRT-PCR) analysis. For chilling treatment, 30-day tomato seedlings were transferred to a growth chamber with a low-temperature (4 °C) environment for 48 h, maintaining light intensity and photoperiod unchanged. Leaf samples for qRT-PCR were collected at 0, 3, 6, 9, 12, 24, and 48 h after chilling treatment. After that, seedlings were transferred to the growth conditions before treatment for 48 h, and recovery (R) leaf samples were collected. Waterlogging treatment

was administered using plastic trays filled with water to fully immerse the entire 30-day tomato seedlings, ensuring that the water level remained less than 1 cm above the apex of the plants. The light intensity, day and night cycle, and growth temperature remained unchanged. Then, after 0, 1, 3, and 5 days of waterlogging treatment, the leaves of tomatoes were collected for RNA extraction and qRT-PCR.

The growth conditions and stress treatment methods for the transgenic plants were maintained consistent with the above description. For chilling treatment, 0 and 48 h leaf samples were used to detect physiological indexes; for waterlogging treatment, 0 and 3 d leaf samples were used.

### 2.3. Gene Clone and qRT-PCR

The RNA extraction process from Micro-Tom leaves involved the utilization of the FlashPure Plant Total RNA Mini Kit (R019, GeneBetter Life Science, Beijing, China) as per the guidelines outlined by the manufacturer. To clone genes, the initial step involved the synthesis of first-strand cDNA using the RevertAid First Strand cDNA Synthesis Kit (K1622, Thermo Scientific, <https://www.thermofisher.cn/>, accessed on 13 May 2024). Primers for gene cloning were designed using Primer Premier 6.0 (Table S1). For qRT-PCR, cDNA synthesis was conducted according to the manuscript instruction of the PrimeScript™ RT Reagent Kit with gDNA Eraser (Perfect Real Time) (RR047A, Takara, <https://www.takarabiomed.com.cn/>, accessed on 13 May 2024). Then, qRT-PCR was conducted with TB Green® Premix Ex Taq™ II FAST qPCR (CN830A, Takara, <https://www.takarabiomed.com.cn/>, accessed on 13 May 2024) via the LightCycler 96/LightCycler 480 System (Roche Diagnostics; Indianapolis, IN, USA). *SIYCTIN* (*Solyc11g005330*) was used as the reference gene. Gene-specific primers are shown in Table S1.

### 2.4. Subcellular Localization

The online resource “Bio-Analytic Resource for Plant Biology” (BAR) at <http://bar.utoronto.ca> (accessed on 13 May 2024) was utilized to anticipate the subcellular localization of the SIYTPs [30].

Subsequently, the coding sequences (CDSs) of *SIYTP8* and *SIYTP9* were cloned into the plant expression vector pCambia2301, with the inclusion of a GFP label. Briefly, the CDSs of genes were firstly amplified with vector construction primers listed in Table S1, and then homologous recombination reactions were conducted with a linearized pCambia2301 empty vector using the Hieff Clone® Universal One Step Cloning Kit (10922ES50, Yeasen, <https://www.yeasen.com/>, accessed on 13 May 2024). Recombinant plasmids were transformed into *E. coli* (DH5α) for amplification and sequencing validation. pCambia2301-SIYTP8, pCambia2301-SIYTP9-1, and pCambia2301-SIYTP9-2 were transformed into *Agrobacterium tumefaciens* (strain GV3101). Tobacco (*Nicotiana benthamiana*) seedlings were grown under a 16 h photoperiod at 22 °C in a growth chamber. Verification of the appropriate *Agrobacterium* strain for infecting 5-week-old tobacco leaves was conducted. After infection and growth for 48 h at 22 °C, the leaf specimens were placed onto glass slides and examined under a fluorescence microscope (Olympus; Japan) equipped with a 20× objective lens. The detailed experimental procedure used is the one outlined in the study by Wang et al. [31].

### 2.5. Tomato Transformation

Recombinant plasmids obtained at 2.4 were applied to the tomato transformation process. Then, the GV3101 strain containing pCambia2301-SIYTP8 and pCambia2301-SIYTP9-2 were used to infect Micro-Tom tomato cotyledons at Shanghai Weidi Biotechnology Co., Ltd. (<https://www.weidibio.com/>, accessed on 13 May 2024). The antibiotic kanamycin (50 mg·L<sup>-1</sup>) was used to screen potential transgenic plants, followed by identification at the DNA level using GUS gene primers (Table S1) [32]. Then, potential transgenic lines displaying a segregation ratio of 3:1 were singled out, and transgenic lines at the homozygous T<sub>3</sub> stage were subsequently validated through qRT-PCR.

## 2.6. Measurement of Stress-Related Physiological Indexes

Relative electrolyte leakage (REL) from leaves was determined following the protocol established by Guo et al. [33] using an electrical conductivity meter (DSS-307; SPSIC, Shanghai, China). The detection of chlorophyll concentration was carried out following the methods established by Wang et al. [34]. Moreover, the concentrations of MDA and H<sub>2</sub>O<sub>2</sub> as well as the activities of SOD, CAT, and POD were tested following the established protocols and using the Malondialdehyde (MDA) Test Kit (MDA-2-Y, Comin, <http://www.cominbio.com/index.html>, accessed on 13 May 2024), Hydrogen Peroxide (H<sub>2</sub>O<sub>2</sub>) Test Kit (H<sub>2</sub>O<sub>2</sub>-2-Y, Comin), Superoxide Dismutase (SOD) Test Kit (SOD-2-Y, Comin), Catalase (CAT) Test Kit (CAT-2-W, Comin), and Peroxidase (POD) Test Kit (POD-2-Y, Comin), respectively.

For MDA concentration testing, 100 mg tomato leaves were ground in the extraction solution. After centrifugation, 0.2 mL of the supernatant was mixed with the reaction solution. After incubation at 95° C for 30 min, measurements of the absorbance at 532 nm (A<sub>532</sub>) and 600 nm (A<sub>600</sub>) were conducted. MDA content can be calculated from the difference between A<sub>532</sub> and A<sub>600</sub>.

For H<sub>2</sub>O<sub>2</sub> concentration testing, 100 mg tomato leaves were ground in the extraction solution. After centrifugation, all the supernatants were combined with the reaction solution and labeled as the test group, and a control group was set up without the addition of any supernatants. After incubation at room temperature for 5 min, their absorbance at 415 nm was measured. The concentration of H<sub>2</sub>O<sub>2</sub> can be calculated from the difference in absorbance at 415 nm between the test group and the control group.

For SOD activity, 100 mg tomato leaves were ground in the extraction solution. After centrifugation, we mixed 50 µL of supernatants with the reaction solution and simultaneously set up a control group without the addition of supernatants. After incubation at room temperature for 30 min, their absorbance at 450 nm was measured. SOD activity can be calculated from the difference in absorbance at 450 nm between the test group and the control group.

For CAT activity, 100 mg tomato leaves were ground in the extraction solution. After centrifugation, the supernatants were retained. First, 150 µL of the supernatants was added to the sample group, added to a reaction solution, and left at room temperature for 10 min; on the other hand, the reaction solution was first added to the control group, followed by the supernatants, and the absorbance value was measured immediately, with the wavelength set at 405 nm. CAT activity can be calculated by determining the difference between the test group and the control group.

For POD activity, 100 mg tomato leaves were ground in the extraction solution. After centrifugation, 50 µL the supernatants and 950 µL of the reaction solution were mixed, and the absorbance values A<sub>1</sub> at 1 min and A<sub>2</sub> at 2 min were recorded at 470 nm (with a time interval of 1 min between A<sub>2</sub> and A<sub>1</sub>). POD activity can be calculated by determining the difference between A<sub>1</sub> and A<sub>2</sub>.

## 2.7. Prediction Transcription Factors and Interacting Proteins

Transcription factors that could bind with *SIYTP* gene promoters and proteins that have interact with SIYTPs were predicted using PlantRegMap and STRING (<https://string-db.org/>, accessed on 13 May 2024), respectively, with *S. lycopersicum* being designated as the target species [35,36].

## 3. Results

### 3.1. *SIYTP* Family Member Identification and Analysis

A total of nine *SIYTP*s were identified via two rounds of BLASTP in the *S. lycopersicum* genome. These *SIYTP* genes were renamed according to their gene IDs (Tables S2 and S3). The largest YTP (*SIYTP5*) had a 706 aa (77.2 KDa) and the smallest one (*SIYTP2*) only had a 369 aa (41.1 KDa). *SIYTP*s were located on five chromosomes. *SIYTP5/9s* were localized on chromosomes 1, *SIYTP4/7s* on chromosomes 2, *SIYTP6* on chromosomes 5, *SIYTP1/2/3s* on

chromosomes 8, and *SIYTP8* on chromosomes 12 (Figure S1). Three *SIYTP* genes, namely *SIYTP1*, *SIYTP2*, and *SIYTP3*, were clustered within a genomic region spanning 200 kb on chromosome 8 (Figure S1).

The evolutionary relationships and classifications of tomato *SIYTP*s were elucidated through a phylogenetic tree constructed using the protein sequences of 13 *AtYTP*s and 9 *SIYTP*s (Figures 1 and S2). Similar to animals, tomato *SIYTP*s were divided into 5 subfamilies, which comprise YTHDFa (*SIYTP5*), YTHDFb (*SIYTP6*), YTHDFc (*SIYTP8/9*), YTHDCa (*SIYTP4/7*), and YTHDCb (*SIYTP1/2/3*). It is worth noting that members of the same subfamily also share similarities in their gene (exon/intron) structures. Overall, tomato *SIYTP* gene family members typically exhibited a range of 6 to 9 exons (Figure S3).

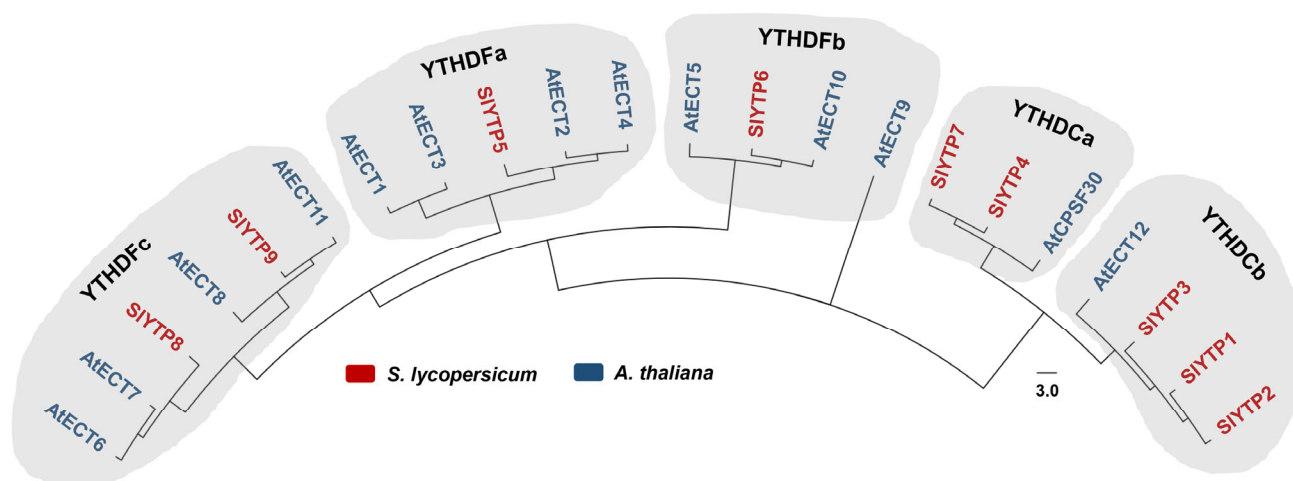


**Figure 1.** Unrooted phylogenetic tree of YTPs from *Solanum lycopersicum* and *Arabidopsis thaliana*. YTPs were divided into five subclasses, YTHDCa, YTHDCb, YTHDFa, YTHDFb, and YTHDFc. The phylogenetic tree was generated utilizing the neighbor-joining algorithm, with 1000 bootstrap iterations used to ascertain the robustness of the tree topology. The scale bar corresponds to a 3.0 genetic distance.

The protein sequence of members of the *SIYTP* family, combined with MEME analysis and protein domain identification, offers valuable information on the evolutionary dynamics of gene families and reinforces the phylogenetic classification (Figures S4–S7). A web-based MEME analysis was conducted to detect novel motifs within the cohort of nine *SIYTP*s. Ten conserved motifs were identified, and each *SIYTP* was found to possess between four and eight of these motifs (Figures S4 and S5). *SIYTP*s in the same subfamily shared similar motifs. Motifs 1/2/3 were included in every *SIYTP*. Others were unique to one or few subclasses. However, all *SIYTP*s contained only one YTH domain. In addition, other protein domains also appeared in these *SIYTP* proteins, i.e., the CPSF30 protein domain (Figure S6). Within the YTHDFa-c subgroup of the *SIYTP* proteins, it was observed that the YTH domain represents the sole identifiable module located at their C-terminus (Figure S6). In the YTHDCa group of the *SIYTP* proteins, they exhibited a YTH domain at their middle region and zinc finger repeats (YTH1 superfamily domain). In the YTHDCb group of the *SIYTP* proteins, they exhibited a YTH domain at their N-terminus region, and *SIYTP2* also exhibited a DUF3568 superfamily domain. YTH domain contained about 110–150 amino acid residues. Sequence alignments revealed that the *SIYTP* protein YTH domains share 69.57% identity. These YTH domains contain three  $\alpha$ -helixes and six  $\beta$ -sheets (Figure S7). In *SIYTP1/2/3/5/6/8/9*, the aromatic cage is constituted by tryptophan residues exclusively, which are denoted as WWW. Conversely, in *SIYTP4/7*, the aromatic cage comprises tryptophan and tyrosine residues, which are noted as WWY. (Figure S7).

The cis-regulatory motifs appeared in the promoter sequences of the *SIYTP*s that were examined. These cis-regulatory elements are associated with environmental stimuli, hormonal signaling pathways, developmental processes, photo-responsive mechanisms,

transcription factor binding sites, and various biological functions. Environmental stress (low temperature, anaerobic stress, drought) and hormone response (ABA, MeJA, SA, GA, auxin) related to cis-acting elements are listed in Figure S8 and Table S4.

### 3.2. Expression Levels of *SIYTPs* in Different Tomato Tissues and under Various Stresses

To confirm the tissue expression of the *SIYTP* genes, their expressions in three different tissues (root, stem, and leaf) were analyzed via qRT-PCR (Figure 2a). The expression levels of all *SIYTPs* are relatively higher in leaves than those in stems and roots. To comprehensively understand the functions of *SIYTPs*, we also downloaded tomato microarray chip data via Genevestigator. The expression data of 14 Micro-Tom tissues/organs at different developmental stages and of 10 Micro-Tom flower and fruit tissues/organs at different developmental stages were included in our analysis. The results revealed that *SIYTP2/3/4/5/9* genes are expressed at different levels in the 14 tissues/organs at different developmental stages, especially *SIYTP9* (Figure S9). In the 10 Micro-Tom flower and fruit tissues/organs at different developmental stages, *SIYTP2/3/5/9* genes are expressed in all these tissues (Figure S10). In addition, *SIYTP2/3/4/5/6/7/8/9* genes exhibit different expression patterns at various tomato growth and developmental stages (Figure S11). The different expression patterns of tomato *SIYTP* genes in different tissues and developmental stages shed light on their functional differences.

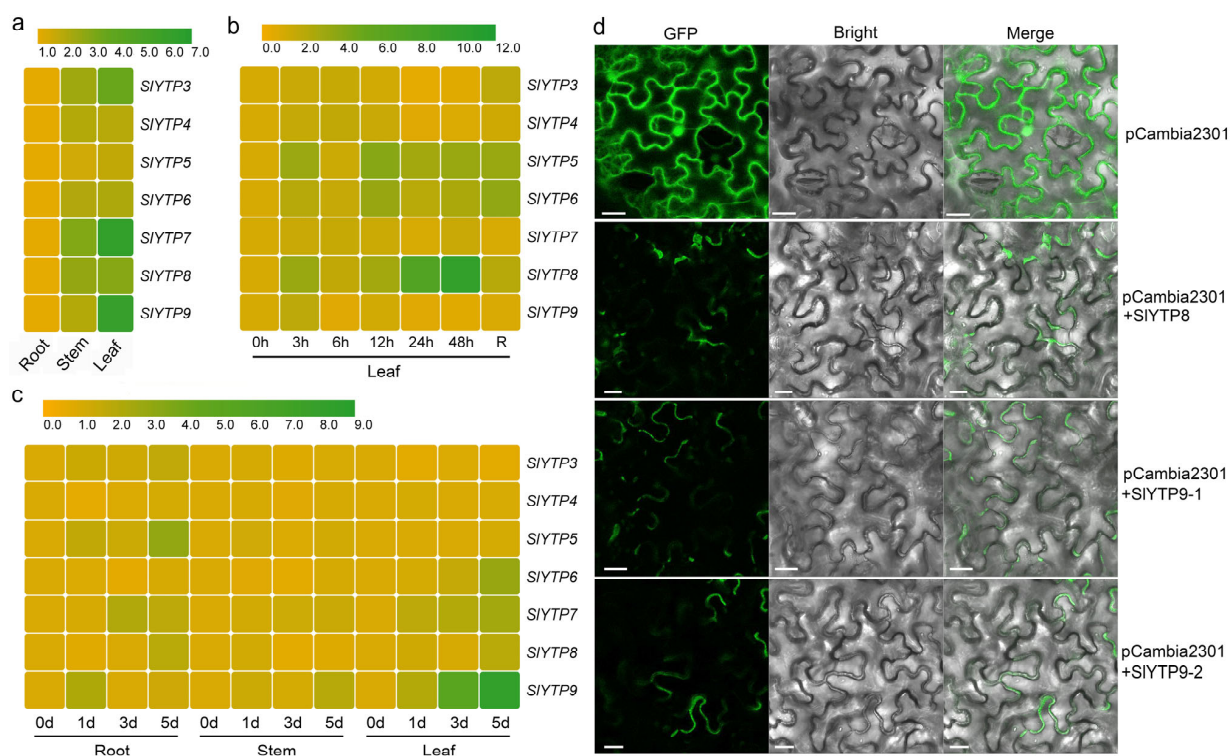


**Figure 2.** Expression patterns of *SIYTP* genes and subcellular localizations of *SIYTP8* and *SIYTP9*. (a) The differential expression levels of representative *SIYTP* genes in tomato roots, stems, and leaves. Scale bar represents relative expression levels. The average expression values were determined based on a minimum of three independent biological replicates and were normalized relative to the expression in root tissues. (b,c) Heatmap showing the expression of *SIYTP* genes in response to low-temperature stress in tomato leaves (b) and in response to waterlogging stress in tomato roots, stems, and leaves (c); scale bar represents relative expression levels. The average expression values were determined from a minimum of three independent biological replicates relative to the expression level at day 0. (d) Subcellular localization of *SIYTP8*, *SIYTP9-1*, and *SIYTP9-2*. Confocal microscopy images of *Nicotiana benthamiana* epidermal leaf cells co-expressing with GFP alone, *SIYTP8*-GFP, *SIYTP9-1*-GFP, and *SIYTP9-2*-GFP, respectively. From left to right, columns show GFP fluorescence, bright-field, and merged images. Scale bars = 20  $\mu\text{m}$ .

To investigate whether *SIYTPs* participate in waterlogging and chilling stresses, wild-type (WT) Micro-Tom tomatoes were treated as described in the Materials and Methods section. Expression levels of *SIYTP3/5/7/8/9* increased in chilling treated leaves (Figure 2b). As Figure 2c shows, *SIYTP3/5/7/8/9* increased expression patterns in waterlogged roots, *SIYTP7/9* in stems, and *SIYTP6/7/8/9* in leaves. Among them, *SIYTP8* and *SIYTP9* genes respond most notable to the low temperature and waterlogging stresses, respectively. To gain an insight into the potential functions of *SIYTPs* under other stress responses, we reviewed the available expression data obtained from the Genevestigator microarray chip experiments database. Regarding N-rich treatment, *SIYTP2/3/4/5/6/9* genes showed decreased expression levels (Figure S12). For NaCl treatment, *SIYTP2/3/4/6/9* genes show increased expression levels and the *SIYTP5* gene shows a decreased expression level (Figure S13). For pathogen infection, *SIYTP2/3/4/6/9* genes showed decreased expression levels (Figure S14). The aforementioned results unveiled variations in the expression levels of the *SIYTP* genes under diverse treatment conditions, suggesting that they probably participate in distinct stress responses. Specifically, *SIYTP8* exhibited heightened expression levels in response to low-temperature stress, while *SIYTP9* displayed prominent expression patterns under waterlogging conditions. The two YTHDFc subgroup genes, *SIYTP8* and *SIYTP9*, were specifically targeted for a detailed examination in the present study due to their notable responsiveness.

We then cloned coding regions of the nine *SIYTP* genes. However, only the *SIYTP3-9* genes that were obtained and aligned with the downloaded sequence from tomato the genome database were analyzed (Table S3). Most of them had a 100% identify fit with the downloaded ones. Interestingly, we obtained two form transcripts of the *SIYTP9* gene. Figure S15 shows the sequence alignment schematic of *SIYTP9*'s two transcripts, *SIYTP9-1* and *SIYTP9-2*, which we cloned from Micro-Tom tomato leaves. The *SIYTP9-2* transcript has a 45 bp length sequence insertion in the 190 bp location, compared to the *SIYTP9-1* transcript. Nevertheless, subcellular localization results showed that *SIYTP8*, *SIYTP9-1*, and *SIYTP9-2* were all present in cytoplasm (Figure 2d), which is in line with the subcellular localization characteristics of the members of the YTHDFc subgroup. Furthermore, bioinformatic analysis based on the *SIYTP3-6* amino acid sequences suggested that all of them could be located on the nucleus (Figure S16).

### 3.3. Overexpression of *SIYTP8* Changes the Chilling Resistance of Tomato

Tomato *SIYTP8*, in the entire *SIYTP* gene family, shows the most significant response to low-temperature stress (Figure 2b). In order to investigate the specific function of *SIYTP8* in the low-temperature stress response, we overexpressed *SIYTP8* in tomatoes (Figure S17) and compared the phenotypes of the overexpressing (OE) lines with those of WT plants after treatment. The *SIYTP8* OE plants and the WT plants exhibit similar phenotypes at normal temperature conditions; however, after 48 h of low-temperature treatment, the OE plants show a more severe leaf curling, indicating that they have a higher sensitivity to cold stress compared to WT plants (Figure 3a). Moreover, to assess membrane damage under low-temperature stress conditions, REL and MDA concentrations in leaves were detected and analyzed. Consistent with the phenotypic results, at a normal temperature condition, there were no significant differences between the *SIYTP8* OE and WT tomato leaves in terms of their REL and MDA content. However, after chilling treatment, both the REL (Figure 3b) and MDA contents (Figure 3c) of the leaves in the *SIYTP8* OE plants were significantly higher than those in WT tomatoes.

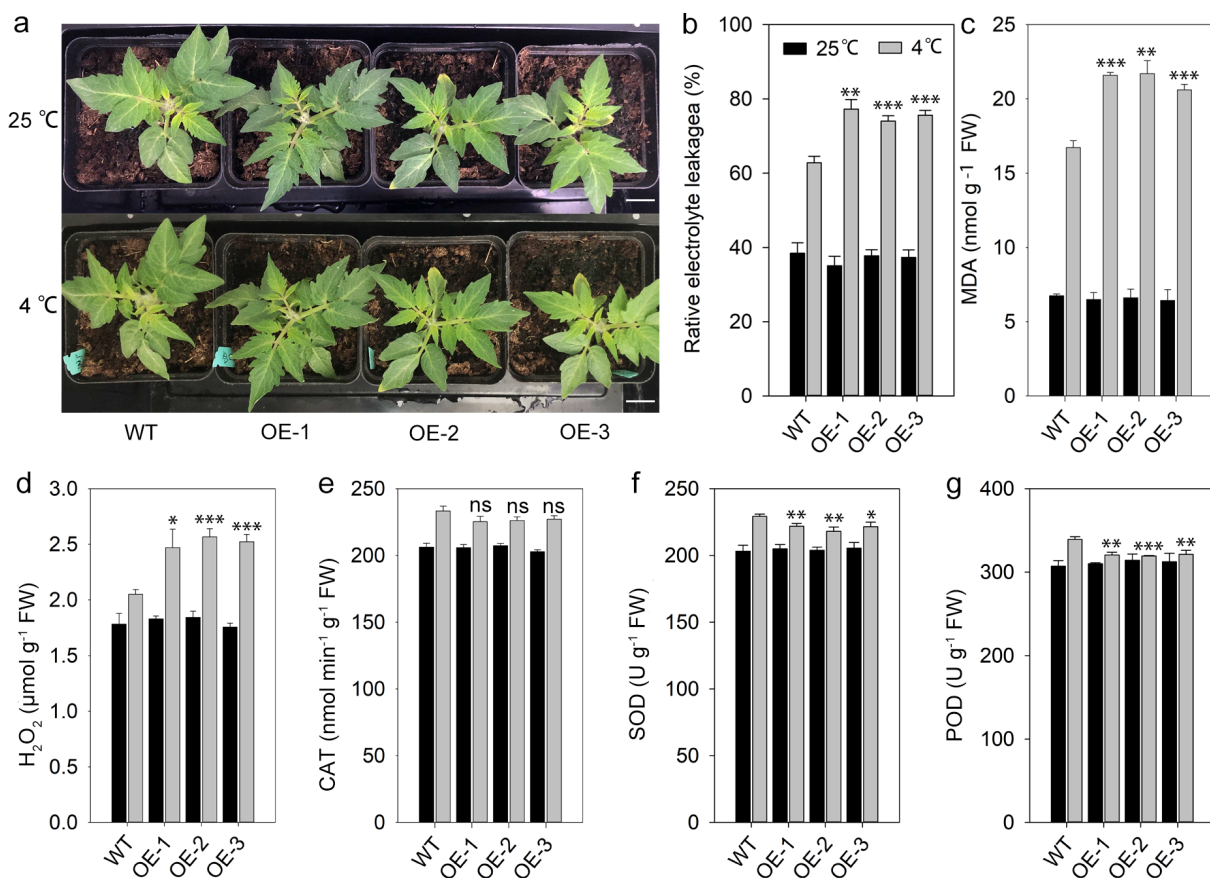


**Figure 3.** Overexpression of the *SIYTP8* gene increased the sensitivity of tomato plants to low-temperature stress. (a) Phenotype of wild-type (WT) and *SIYTP8* overexpression (OE) lines under 25 °C and 4 °C conditions. Scale bars = 2 cm. (b–g) Stress-related physiological index measurements, including relative electrolyte leakage (REL) (b), malondialdehyde (MDA) concentration (c), hydrogen peroxide (H<sub>2</sub>O<sub>2</sub>) concentration (d), catalase (CAT) activity (e), superoxide dismutase (SOD) activity (f), and peroxidase (POD) activity (g). Error bars indicate the standard error of three biological replicates. \*, \*\*, \*\*\*, and ns (no significance) are indicated by  $p < 0.05$ ,  $p < 0.01$ ,  $p < 0.001$ , and  $p > 0.05$  (two tailed *t*-test), respectively.

Low-temperature stress has been observed to trigger the accumulation of reactive oxygen species (ROS) within plant tissues and cells, leading to oxidative damage. As Figure 3d shows, the accumulation of H<sub>2</sub>O<sub>2</sub> in OE plants is significantly higher than that in WT leaves. However, in relation to the enzymatic activities of the three enzymes related to the removal of reactive oxygen species, although there is no significant difference in CAT activity between OE and WT plants (Figure 3e), the activities of SOD and POD in transgenic plant lines are significantly lower than those in WT tomatoes (Figure 3f,g). It is worth noting that there are no significant differences in the H<sub>2</sub>O<sub>2</sub> content and activity of the three enzymes between OE and WT tomatoes under normal conditions (Figure 3d–g). The above experimental results further indicate that tomatoes the overexpress the *SIYTP8* gene are more sensitive to low temperatures than WT plants, with a greater accumulation of oxidative substances and weaker reactive oxygen species' scavenging ability.

Meanwhile, the effect of *Arabidopsis* *YTP* genes on trichome development prompted us to investigate the impact of *SIYTP8* gene expression on tomato trichomes [13]. WT and *SIYTP8* transgenic tomato cotyledons and true leaves were collected for a microscopic observation of the number and length of trichomes on the epidermis (Figure S18a). After statistical analysis, it was found that the length of trichomes on the cotyledons of OE lines showed no significant difference compared to those of WT tomatoes (Figure S18b). However, there was a significant decrease in the number of trichomes on the midsection

of the cotyledons in *SIYTP8* OE plants (Figure S18c). In addition, we also measured the length of trichomes on the midsection of their true leaves. Compared to the WT plants, the *SIYTP8* transgenic tomatoes showed a significant decrease in trichome length on true leaves (Figure S18d). Therefore, the overexpression of *SIYTP8* gene leads to a reduction in trichome length and density, which can be considered as one of the morphological reasons for the decreased chilling resistance in tomatoes that overexpress *SIYTP8*.

### 3.4. Overexpression of *SIYTP9-2* Increases Waterlogging Resistance of Tomatoes

In the waterlogging stress treatment conducted in this study, the *SIYTP9* gene showed the most pronounced response. For genes with multiple transcript variants, the longest transcript is often considered the primary transcript. Thus, three OE tomato lines of *SIYTP9-2* genes were obtained through genetic transformation (Figure S17). After waterlogging treatment, WT plants exhibited a higher degree of leaf yellowing compared to *SIYTP9-2* OE tomatoes (Figure 4a,b). Figure 4c also indicates that the accumulation of MDA in transgenic plants after waterlogging treatment is significantly lower than that in WT plants, although there is no significant difference between *SIYTP9* OE-1 plants and WT tomatoes, which may be caused by the lower *SIYTP9-2* overexpression levels comparing to OE-2 and -3 lines (Figures 4c and S17).

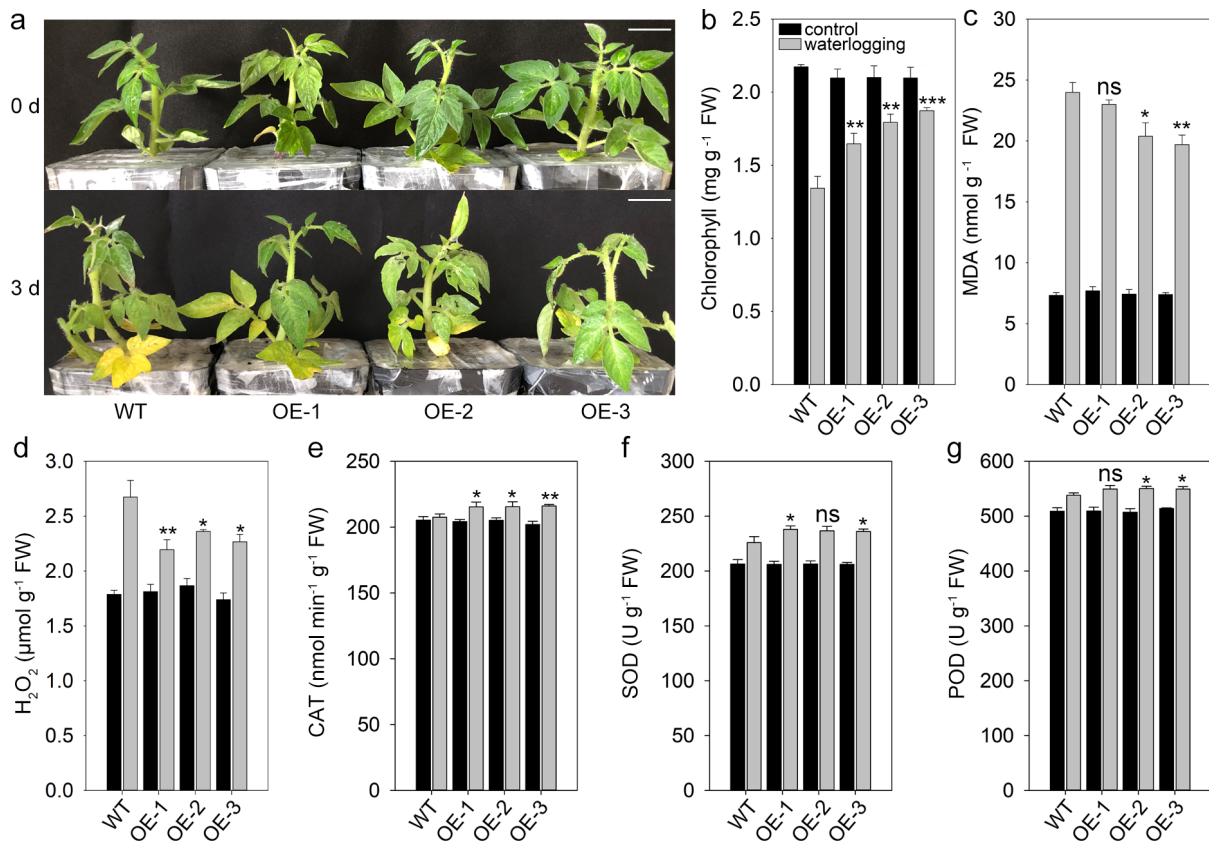


**Figure 4.** Overexpression of the *SIYTP9-2* gene increased the resistance of tomato plants to waterlogging stress. (a) Phenotype of WT and *SIYTP9-2* OE lines under normal and waterlogging stress conditions. Scale bars = 2 cm. (b–g) Stress-related physiological index measurements, including chlorophyll concentration (b), MDA concentration (c), H<sub>2</sub>O<sub>2</sub> concentration (d), CAT activity (e), SOD activity (f), and POD activity (g). Error bars indicate the standard error of three biological replicates. \*, \*\*, \*\*\*, and ns (no significance) are indicated by  $p < 0.05$ ,  $p < 0.01$ ,  $p < 0.001$ , and  $p > 0.05$  (two tailed  $t$ -test), respectively.

Similarly, in terms of the accumulation and scavenging of ROS, there was no significant difference between *SIYTP9-2* OE and WT tomatoes under normal growth conditions. However, after waterlogging treatment, the OE lines showed a significantly lower ROS accumulation and a significantly higher ROS scavenging capacity compared to WT plants, with a lower hydrogen peroxide accumulation and higher CAT, SOD, and POD activities (Figure 4d–g). Although there was no significant difference in the activities of SOD and POD enzymes in the leaves of the OE-1 and OE-2 plants, respectively, compared to WT tomatoes after waterlogging treatment (Figure 4f,g), the above experimental results still indicate that the overexpression of the *SIYTP9* gene enhances the tomato plant's resistance to waterlogging stress to some extent.

### 3.5. Prediction of Transcription Factors Binding with *SIYTP8* or *SIYTP9* Promoter and Interaction Proteins of *SIYTP8* and *SIYTP9*

The cis-acting elements modulate the accurate onset and efficacy of gene transcription by interacting with TFs. Therefore, we predicted the potential TFs which may regulate the transcription of *SIYTPs* (Figure 5a, Table S5). Figure 5a shows the predicted transcription factors of *SIYTP8* and *SIYTP9*. For *SIYTP8*, there are four key TFs, including two MYB TFs, one ARF family protein, and one Dof family protein, which are related to plant hormone (auxin, SA, and ABA) signaling and abiotic stress (salt and drought) responses. Regarding *SIYTP9*, there are three TFs, including one MYB TF, one ARF family protein, and one NAC family protein, which are related to auxin signaling, ABA signaling, and cold stress responses. The prediction of TFs binding to promoters and their potential involvement in stress or external stimuli further reflects the functions of *SIYTP8* and *SIYTP9* in response to adverse stresses.

Proteins always need to interact with other proteins to perform their functions. Therefore, we predicted the potential interaction proteins of *SIYTPs* and constructed a protein–protein interaction (PPI) network of *SIYTP8* and *SIYTP9* (Figure 5b, Table S6). We discovered that there are 12 proteins (P1–12) that have a relationship with *SIYTP8* or *SIYTP9* (Figure 5b). Among them, P1–P5 indirectly interact with *SIYTP9*, and most of them (P2–P4) are RNA helicase; P6–8 proteins both interact with *SIYTP9* and *SIYTP8*. P6–7 are 3′-5′-exoribonuclease family proteins, and P8 is a ubiquitin-specific protease. P9–12 could only interact with *SIYTP8*, and P9–10 are mRNA methylation-related proteins. P11–12 are related to post-transcription and protein translation processes, with P11 being poly(A)-specific ribonuclease and P12 being a negative translation regulator. These results indicate that *SIYTP8* and *SIYTP9*, as m<sup>6</sup>A readers, can participate in many RNA co- and post-transcription-level regulatory processes, such as RNA helicase, mRNA methylation, and RNA decay.

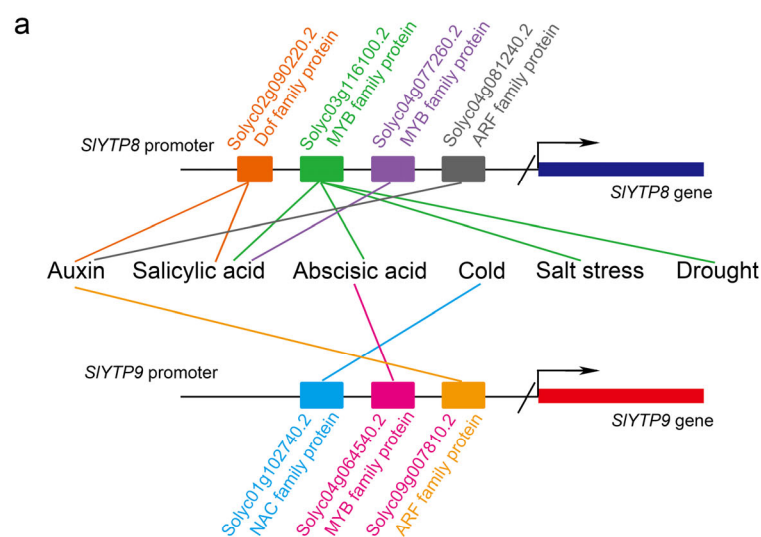
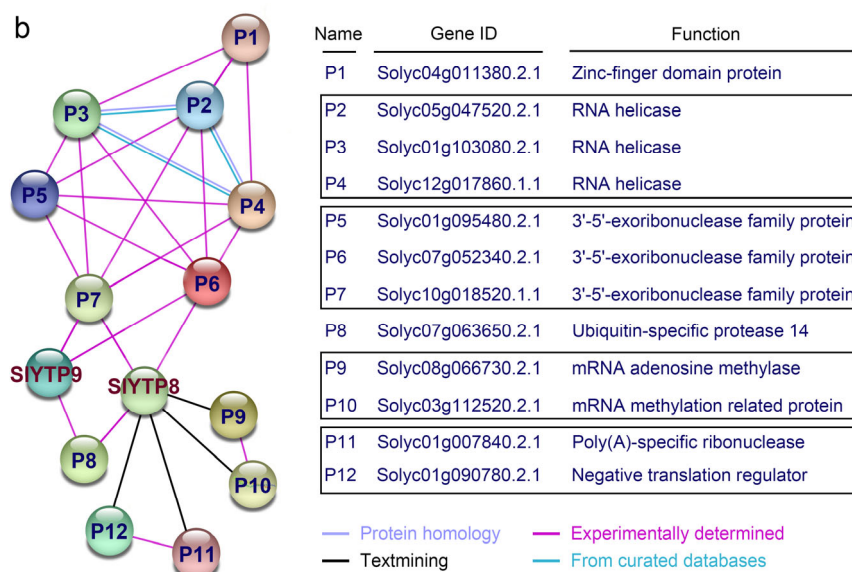


Figure 5. Cont.



**Figure 5.** Predicted gene expression networks of SIYTP8 and SIYTP9. (a) Predicted transcription factors (TFs) binding with *SIYTP8* or *SIYTP9* promoters. Black lines represent promoters. Dark blue and red strips represent genes. Colored rectangles represent predicted TFs binding with promoters. Lines with the same color link phytohormones or stresses with these TFs, indicating that each TF can influence gene expressions under specific phytohormone stimulation and/or stress conditions. (b) Predicted interacting proteins of SIYTP8 and SIYTP9. Regulation network between SIYTP8/9 and potential binding proteins is shown on the left. Table on the right lists gene IDs and the functions of these proteins. Interactions among them are obtained from protein homology, experiments, text mining, and/or from curated databases, which are presented by different colored lines.

## 4. Discussion

### 4.1. SIYTP Family Member Identification and Analysis

In line with previous studies, there are nine *SIYTP* members in the tomato genome, which are all divided into five subcategories (YTHDFa-c and YTHDCa-b), although they are named differently (Figure 1) [15,37]. Moreover, YTP family members can also be divided into these five subfamilies in *Arabidopsis* (*A. thaliana*) [13], apple (*Malus domestica*) [38], and alfalfa (*Medicago sativa*) [39]. Nevertheless, not all plants contain all the YTP subgroup members. The absence of YTHDCb proteins in common wheat and rice is in accordance with the previous hypothesis that there are no group-b YTHDCs in the monocotyledon lineage, indicating that this version of the YTH motif was lost in the common ancestor of monocotyledons [16,40].

Moreover, the positioning of the YTH domain in YTP sequences also exhibits differences between tomatoes and animals. The most significant disparity is manifested by the YTH domain of tomato YTHDCb subclass SIYTPs (SIYTP1/2/3) being located at their N-terminus, while the YTH domain is located at the C-terminus of human YTHDCb (Figure S6) [12]. Human YTHDCb is also characterized by the presence of a DEAD-box RNA helicase domain, which facilitates the unwinding of 5'-UTR regions and enhances the translational efficacy of the respective gene [41,42]. In the plant kingdom, YTPs containing the DEAD-box RNA helicase domain have not been reported. Consequently, it remains uncertain whether the unwinding activity associated with YTPs is essential for their recognition of the m<sup>6</sup>A modification. Nevertheless, the tomato SIYTP4 protein contains a Cytadhesin P30 superfamily domain, which determines its function in the control and choice of the polyadenylation site [43].

The YTH structural domain is crucial for the recognition of m<sup>6</sup>A modifications, as it specifically recognizes and interacts with methylated adenosine by means of an aromatic cage created by its critical amino acid residues [11,44]. In human YTHDFa, the positively

charged pocket is constructed by the side chains of tryptophan (W411), tryptophan (W465), and tryptophan (W470) [11]. In this study, we found that the aromatic cage in YTHDFa-c subclass SIYTPs (SIYTP5/6/8/9) and that in YTHDCb subclass SIYTPs (SIYTP1/2/3) comprises WWW (Figure S7). On the other hand, the aromatic cage is formed by tryptophan (W377), tryptophan (W428), and leucine (L439) in human YTHDCa [11]. However, the cage in the YTHDCa subclass SIYTPs (SIYTP4/7) comprises WWY (Figure S7). The analyses suggested that plant YTHDCs may exhibit distinct m<sup>6</sup>A-binding characteristics compared to animal YTHDCs.

#### 4.2. Expression Patterns of *SIYTP8* and Its Function in Tomato Low-Temperature Stress Resistance

The expression level of *SIYTP8* is higher in tomato stems and leaves than in the roots (Figure 2a). The expression trend of *SIYTP8* in roots, stems, and leaves is consistent in the literature [37]. Moreover, its expression level in flowers and fruits is even higher than in stems and leaves, indicating that it plays a role in the function of reproductive organs of tomatoes [37]. *SIYTP8*, as a member of the YTHDFc subfamily, has a subcellular localization in the cytoplasm (Figure 2d). In mammals, subcellular localizations vary among members of different subclasses, with the YTHDCa subclass members being localized in the cell nucleus, while members of other subclasses (YTHDCb and YTHDFa-c) can all be detected in the cytoplasm [45]. Arabidopsis AtECT2, AtECT3, and AtECT4 are extensively studied m<sup>6</sup>A readers, which play important biological roles in leaf development and stem elongation processes as well as being the members of the YTHDFa subclass, and they are all localized in the cytoplasm [13,17,46]. Moreover, AtCPSF30-L is a protein localized within the nucleus. It exhibits the capacity to identify and interact with precursor RNAs containing m<sup>6</sup>A modifications, subsequently modulating the polyadenylation process [44].

Besides acting as the RNA m<sup>6</sup>A modification reader, Arabidopsis ECT2 plays an indispensable role in the normal development of trichomes in the leaf epidermis [40]. Although the overexpression of tomato *SIYTP8* does not affect the morphology of the tomato leaf trichome, it alters the length or density trichome in the cotyledon or true leaves (Figure S18). Tomato *SIYTP8*, in the entire *SIYTP* gene family, shows the most significant response to low-temperature stress (Figure 2b), and its overexpression makes it more sensitive to cold stress in tomatoes (Figure 3). We speculate that the low-temperature sensitive phenotype is to some extent caused by the changes in the density and length of surface trichomes.

Similarly, Shen et al. also pointed out that the expression level of the *SIYTP8* (*SIYTHDF3B*) gene significantly increased after 48 h of low-temperature treatment and was also significantly upregulated after heat treatment [15]. Moreover, Yin et al. reported that *SIYTP8* (*SIYTH4*) has a downregulated expression after ABA treatment and an unregulated expression after MeJA treatment [37]. *AtYTH10* (*At3G17330*, *AtECT6*) is the homology gene of *SIYTP8* in Arabidopsis, which has a heat stress response expression pattern [14]. Moreover, other Arabidopsis YTP members (*At1g79270*; *AtECT8*) also show significant upregulated expression levels in low-temperature conditions [14]. In alfalfa (*Medicago sativa*), the most significant increase in the expression of *MsYTH* occurs in *MsYTH2* and *MsYTH14* under cold stress, whereas under salinity conditions, *MsYTH2* is predominantly expressed [39]. Moreover, not only do m<sup>6</sup>A readers exhibit a relationship with the chilling stress response but also the m<sup>6</sup>A modification. For example, Vicente et al. characterized diverse functions of the cellular m<sup>6</sup>A RNA methylome in adapting to cold stress, with a predominant focus on chloroplasts, where it played a crucial role in maintaining photosynthetic stability [47]. Wang et al. elucidated the pivotal contribution of the m<sup>6</sup>A modification in modulating growth under low-temperature conditions and proposed a potential mechanism involving translational regulation in Arabidopsis's response to low-temperature stress [48].

#### 4.3. Expression Patterns of *SIYTP9-2* and Its Function in Tomato Waterlogging Stress Resistance

There are two transcripts of *SIYTP9*—*SIYTP9-1* and *SIYTP9-2*—which suggests that there may be alternative splicing events after *SIYTP9* gene transcription (Figure S15). Due to the principled nature of the quantitative design of their primers, it is impossible to distinguish the expression levels of the two transcripts; thus, the gene expression of *SIYTP9* represents the expression levels of the two transcripts. The expression level of the *SIYTP9* gene gradually increases in the roots, stems, and leaves (Figure 2c). The expression pattern of the *SIYTP9* (*SIYTHDF3A*) gene, as reported by Shen et al., also shows a gradual increase in the roots, stems, and leaves. Moreover, it was exhibited the highest expression level is in immature fruits [15]. However, Yin et al. reported that its highest expression levels occur in the roots, among all the tissue/organs that were detected, which may be caused by differences in the growth status of the plants [37]. Neither of these studies found the two transcripts of *SIYTP9*. As a member of the YTHDFc subfamily, *SIYTP9*, is also localized in the cytoplasm (Figure 2d). Furthermore, *SIYTP9-1* and *SIYTP9-2* display no differences in their subcellular localizations, indicating that there may be some functional relevance and complementarity present between them.

After waterlogging stress treatment was conducted in this study, the *SIYTP9* gene showed the most pronounced response (Figure 2c). Additionally, the overexpression of *SIYTP9-2* gene enhanced the plant's resistance to waterlogging stress (Figure 4). Yin et al. reported that *SIYTP9* (*SIYTH1*) could respond to GA<sub>3</sub> treatment [37]. Moreover, Shen et al. also found that *SIYTP9* (*SIYTHDF3A*) does not respond to cold treatment, but its expression increases significantly after heat treatment [15]. In line with the literature, the homologous gene of *SIYTP9* in *Arabidopsis thaliana*, *AtYTH6* (*At1g79270*; *AtECT8*), is able to respond to osmotic stress, besides high salinity treatment [14]. For other *YTPs*, both apple *MhYTP1* and *MhYTP2* can be induced by various stresses, e.g., waterlogging, water deficits, and high salinity [49].

#### 4.4. Prediction of Transcription Factors Binding with *SIYTP8* or *SIYTP9* Promoter and Interaction Proteins of *SIYTP8* and *SIYTP9*

There are numerous predicted TFs that can bind with the promoters of *SIYTP8* or *SIYTP9*, which can respond to phytohormones and abiotic stress, such as cold, drought, and high salinity stresses (Figure 5a). The prediction of transcription factors binding to promoters and their potential involvement in stress or external stimuli further reflects the functions of *SIYTP8* and *SIYTP9* in response to adverse stresses.

Moreover, among the potential interaction proteins of *SIYTPs* and the constructed PPI network, P9–12 could only interact with *SIYTP8*, with P9–10 being mRNA methylation-related proteins. P11–12 are related to post-transcription and protein translation processes, with P11 being poly(A)-specific ribonuclease and P12 being a negative translation regulator (Figure 5b). In *Arabidopsis thaliana*, the m<sup>6</sup>A methyltransferase complex consists of two core methyltransferases, mRNA adenosine methylase (MTA) and MTB, along with various accessory subunits including FK506-BINDING PROTEIN 12 KD INTERACTING PROTEIN 37KD (FIP37), VIRILIZER (VIR), and HAKAI [50]. P9 (*solyc08g066730*) is the core subunit of the m<sup>6</sup>A writer, MTA, which can catalyze the methylation of specific adenosine sites on mRNA. P10 (*Solyc03g112520*) is FIP37. Consequently, Shen et al. also revealed that FIP37 and VIR play a crucial role in stabilizing the methyltransferases MTA and MTB within the m<sup>6</sup>A methyltransferase complex, serving as essential subunits for sustaining the complex's functionality [50].

P11–12 are both CCR4-NOT transcription complex subunits. P11 is CCR4-associated factor 1. In both yeast and mammals, the CAF1 protein is a member of the evolutionarily conserved CCR4-NOT complex, which serves a crucial function in regulating transcription and mRNA degradation [51]. In *Capsicum annuum*, CaCAF1 is essential for both plant development and defense mechanisms [52]. Similar to this is AtCAF1 in *A. thaliana*, which also plays a role in plant development and defense mechanisms, while exhibiting mRNA deadenylating activity [52]. P12 is the CCR4-NOT complex component NOT1 and acts

as a scaffold protein in the CCR4-NOT complex, and it obtains such a role by interacting with various NOT proteins and CAF1. Arabidopsis NOT1 (AtNOT1) is involved in modulating RNA-directed DNA methylation and transcriptional silencing through its role in promoting Pol IV-mediated siRNA generation [53]. Additionally, AtNOT1 is a crucial protein required for the correct development of pollen and has the capacity for conducting germination [54,55].

The predicted protein–protein interaction results above indicate that SIYTP8 and SIYTP9, as readers of m<sup>6</sup>A, can recognize m<sup>6</sup>A modifications on RNA and interact with RNA m<sup>6</sup>A methylation and post-transcription-related proteins, thereby modifying the expression levels of specific target genes in response to external environmental stimuli and stress signals.

## 5. Conclusions

In this study, nine *SIYTPs* were identified in tomatoes (*S. lycopersicum*) and could be divided into five subclasses. Among them, *SIYTP8* and *SIYTP9*, as members of the YTHDFc subfamily, could respond to cold and waterlogging stress, respectively. Furthermore, the overexpression of *SIYTP8* or *SIYTP9* could alter the resistance of tomatoes to corresponding stress. The predicted protein–protein interaction results indicate that *SIYTP8* and *SIYTP9*, as readers of m<sup>6</sup>A, can recognize m<sup>6</sup>A modifications on RNA and are predicted to be able to interact with RNA m<sup>6</sup>A methylation and post-transcription-related proteins, thereby altering the expression of target genes in response to external environmental and stress signals. A detailed molecular mechanism is worth exploring and verifying with further experiments. Future research should focus on the functions of *SIYTP8* and *SIYTP9* in other stress responses, functional differences of the two transcripts of the *SIYTP9* gene, as well as the potential roles of other *SIYTPs* in plant stress resistance.

**Supplementary Materials:** The following supporting information can be downloaded at: <https://www.mdpi.com/article/10.3390/horticulturae10050522/s1>, Figure S1: Chromosomal distributions and gene duplications of *SIYTP* genes in tomato genome. Figure S2: Unrooted phylogenetic tree of YTPs from *S. lycopersicum*. Figure S3: Phylogenetic relationship and gene structure of *SIYTPs*. Figure S4: Phylogenetic relationship and architecture of the conserved protein motifs in *SIYTPs*. Figure S5: Motif sequence information. Figure S6: Phylogenetic relationship and conserved protein domains in *SIYTPs*. Figure S7: Multiple sequence alignment of the YTH domain of *SIYTPs*. Figure S8: Phylogenetic relationship and prediction of cis-acting elements in *SIYTP* promoters. Figure S9: Analysis of expression pattern of *SIYTP2/3/4/5/6/9* in different tissues/organs of Micro-Tom using Genevestigator. Figure S10: Analysis of expression patterns of *SIYTP2/3/4/5/6/9* in different flower/fruit development stage of Micro-Tom using Genevestigator. Figure S11: Analysis of expression pattern of *SIYTP2/3/4/5/6/9* in different development stage of tomato using Genevestigator. Figure S12: Analysis of expression pattern of *SIYTP2/3/4/5/6/9* under high NH<sub>4</sub><sup>+</sup> condition in tomato root using Genevestigator. Figure S13: Analysis of expression pattern of *SIYTP2/3/4/5/6/9* under high NaCl condition in tomato using Genevestigator. Figure S14: Analysis of expression pattern of *SIYTP2/3/4/5/6/9* after pathogen infection in tomato leaf using Genevestigator. Figure S15: Sequence alignment schematic of *SIYTP9* two transcripts. Figure S16: Prediction subcellular localizations of *SIYTP3/4/5/6/7*. Figure S17: Expression levels of *SIYTP8* and *SIYTP9-2* in WT and overexpression of transgenic tomato plants. Figure S18: Observation of trichomes in the epidermis of WT and *SIYTP8* transgenic tomatoes leaves. Table S1: Primers used in this study. Table S2: Information of *SIYTP* genes and the predicated proteins in *Solanum lycopersicum*. Table S3: Sequences of *SIYTPs* downloaded from tomato genome database and obtained from gene cloning. Table S4: The numerical and functional data for each cis-acting element in *SIYTP* promoters. Table S5: Predicted transcription factors binding with promoters of *SIYTP4/5/6/7*. Table S6: Predicted interaction proteins of *SIYTP3/4/5/6/7*.

**Author Contributions:** N.W. and L.J. initiated and designed the experiments; Y.Z., T.G. and J.L. performed the experiments and collected the data; N.W. analyzed the data and wrote the manuscript; N.W. and L.J. revised the manuscript. All authors have read and agreed to the published version of the manuscript.

**Funding:** This work was financially supported by the National Natural Science Foundation of China (Grant No. 32202518) and the Shandong University of Technology PhD Start-up Fund (418097).

**Data Availability Statement:** The original contributions presented in the study are included in the Supplementary Materials, further inquiries can be directed to the corresponding author.

**Acknowledgments:** We express our gratitude to Fengwang Ma for generously providing us with Micro-Tom seeds.

**Conflicts of Interest:** The authors declare no conflicts of interest.

## Abbreviations

YT521-B homology (YTH); YTH domain-containing RNA-binding proteins (YTPs); *N*<sup>6</sup>-methyladenosine (m<sup>6</sup>A); wild type (WT); overexpression (OE); relative electrolyte leakage (REL); malondialdehyde (MDA); hydrogen peroxide (H<sub>2</sub>O<sub>2</sub>); catalase (CAT); superoxide dismutase (SOD); peroxidase (POD); *N*<sup>1</sup>-methyladenosine (m<sup>1</sup>A); *N*<sup>4</sup>-acetylcytidine (ac<sup>4</sup>C); YTH domain-containing protein (YTHDC); YTH domain-containing family protein (YTHDF); salicylic acid (SA); molecular weights (MWs); quantitative real time polymerase chain reaction (qRT-PCR); reactive oxygen species (ROS); transcription factors (TFs); protein–protein interaction (PPI).

## References

- Wiener, D.; Schwartz, S. The epitranscriptome beyond m<sup>6</sup>A. *Nat. Rev. Genet.* **2021**, *22*, 119–131. [[CrossRef](#)] [[PubMed](#)]
- Ramakrishnan, M.; Rajan, K.S.; Mullasser, S.; Ahmad, Z.; Zhou, M.; Sharma, A.; Ramasamy, S.; Wei, Q. Exploring *N*<sup>6</sup>-methyladenosine (m<sup>6</sup>A) modification in tree species: Opportunities and challenges. *Hortic. Res.* **2023**, *11*, uhad284. [[CrossRef](#)] [[PubMed](#)]
- Song, P.; Cai, Z.; Jia, G. Principles, functions, and biological implications of m<sup>6</sup>A in plants. *RNA* **2024**, *30*, 491–499. [[CrossRef](#)] [[PubMed](#)]
- Frye, M.; Harada, B.T.; Behm, M.; He, C. RNA modifications modulate gene expression during development. *Science* **2018**, *361*, 1346–1349. [[CrossRef](#)] [[PubMed](#)]
- Song, P.; Tayier, S.; Cai, Z.; Jia, G. RNA methylation in mammalian development and cancer. *Cell Biol. Toxicol.* **2021**, *37*, 811–831. [[CrossRef](#)] [[PubMed](#)]
- Wang, X.; Lu, Z.; Gomez, A.; Hon, G.C.; Yue, Y.; Han, D.; Fu, Y.; Parisien, M.; Dai, Q.; Jia, G.; et al. *N*<sup>6</sup>-methyladenosine-dependent regulation of messenger RNA stability. *Nature* **2014**, *505*, 117–120. [[CrossRef](#)]
- Wang, X.; Zhao, B.S.; Roundtree, I.A.; Lu, Z.; Han, D.; Ma, H.; Weng, X.; Chen, K.; Shi, H.; He, C. *N*<sup>6</sup>-methyladenosine Modulates Messenger RNA Translation Efficiency. *Cell* **2015**, *161*, 1388–1399. [[CrossRef](#)]
- Xiao, W.; Adhikari, S.; Dahal, U.; Chen, Y.S.; Hao, Y.J.; Sun, B.F.; Sun, H.Y.; Li, A.; Ping, X.L.; Lai, W.Y.; et al. Nuclear m<sup>6</sup>A Reader YTHDC1 Regulates mRNA Splicing. *Mol. Cell* **2016**, *61*, 507–519. [[CrossRef](#)] [[PubMed](#)]
- Shi, H.; Wang, X.; Lu, Z.; Zhao, B.S.; Ma, H.; Hsu, P.J.; Liu, C.; He, C. YTHDF3 facilitates translation and decay of *N*<sup>6</sup>-methyladenosine-modified RNA. *Cell Res.* **2017**, *27*, 315–328. [[CrossRef](#)]
- Wojtas, M.N.; Pandey, R.R.; Mendel, M.; Homolka, D.; Sachidanandam, R.; Pillai, R.S. Regulation of m<sup>6</sup>A Transcripts by the 3′→5′ RNA Helicase YTHDC2 Is Essential for a Successful Meiotic Program in the Mammalian Germline. *Mol. Cell* **2017**, *68*, 374–387. [[CrossRef](#)]
- Liao, S.; Sun, H.; Xu, C. YTH Domain: A Family of *N*<sup>6</sup>-methyladenosine (m<sup>6</sup>A) Readers. *Genom. Proteom. Bioinform.* **2018**, *16*, 99–107. [[CrossRef](#)]
- Meyer, K.D.; Jaffrey, S.R. Rethinking m<sup>6</sup>A Readers, Writers, and Erasers. *Annu. Rev. Cell Dev. Biol.* **2017**, *33*, 319–342. [[CrossRef](#)] [[PubMed](#)]
- Arribas-Hernández, L.; Bressendorff, S.; Hansen, M.H.; Poulsen, C.; Erdmann, S.; Brodersen, P. An m<sup>6</sup>A-YTH Module Controls Developmental Timing and Morphogenesis in Arabidopsis. *Plant Cell* **2018**, *30*, 952–967. [[CrossRef](#)] [[PubMed](#)]
- Li, D.; Zhang, H.; Hong, Y.; Huang, L.; Li, X.; Zhang, Y.; Ouyang, Z.; Song, F. Genome-wide identification, biochemical characterization, and expression analyses of the YTH domain-containing RNA-binding protein family in Arabidopsis and rice. *Plant Mol. Biol. Rep.* **2014**, *32*, 1169–1186. [[CrossRef](#)]
- Shen, H.; Luo, B.; Wang, Y.; Li, J.; Hu, Z.; Xie, Q.; Wu, T.; Chen, G. Genome-Wide Identification, Classification and Expression Analysis of m<sup>6</sup>A Gene Family in *Solanum lycopersicum*. *Int. J. Mol. Sci.* **2022**, *23*, 4522. [[CrossRef](#)]
- Sun, J.; Bie, X.M.; Wang, N.; Zhang, X.S.; Gao, X.Q. Genome-wide identification and expression analysis of YTH domain-containing RNA-binding protein family in common wheat. *BMC Plant Biol.* **2020**, *20*, 351. [[CrossRef](#)] [[PubMed](#)]
- Wei, L.H.; Song, P.; Wang, Y.; Lu, Z.; Tang, Q.; Yu, Q.; Xiao, Y.; Zhang, X.; Duan, H.C.; Jia, G. The m<sup>6</sup>A Reader ECT2 Controls Trichome Morphology by Affecting mRNA Stability in Arabidopsis. *Plant Cell* **2018**, *30*, 968–985. [[CrossRef](#)]

18. Arribas-Hernández, L.; Rennie, S.; Schon, M.; Porcelli, C.; Enugutti, B.; Andersson, R.; Nodine, M.D.; Brodersen, P. The YTHDF proteins ECT2 and ECT3 bind largely overlapping target sets and influence target mRNA abundance, not alternative polyadenylation. *eLife* **2021**, *10*, e72377. [[CrossRef](#)]
19. Song, P.; Wei, L.; Chen, Z.; Cai, Z.; Lu, Q.; Wang, C.; Tian, E.; Jia, G. m<sup>6</sup>A readers ECT2/ECT3/ECT4 enhance mRNA stability through direct recruitment of the poly(A) binding proteins in Arabidopsis. *Genome Biol.* **2023**, *24*, 103. [[CrossRef](#)]
20. Lee, K.P.; Liu, K.; Kim, E.Y.; Medina-Puche, L.; Dong, H.; Di, M.; Singh, R.M.; Li, M.; Qi, S.; Meng, Z.; et al. The m<sup>6</sup>A reader ECT1 drives mRNA sequestration to dampen salicylic acid-dependent stress responses in Arabidopsis. *Plant Cell* **2024**, *36*, 746–763. [[CrossRef](#)]
21. Guo, T.; Liu, C.; Meng, F.; Hu, L.; Fu, X.; Yang, Z.; Wang, N.; Jiang, Q.; Zhang, X.; Ma, F. The m<sup>6</sup>A reader *MhYTP2* regulates MdMLO19 mRNA stability and antioxidant genes translation efficiency conferring powdery mildew resistance in apple. *Plant Biotechnol. J.* **2022**, *20*, 511–525. [[CrossRef](#)] [[PubMed](#)]
22. Yin, S.; Ao, Q.; Qiu, T.; Tan, C.; Tu, Y.; Kuang, T.; Yang, Y. Tomato SIYTH1 encoding a putative RNA m<sup>6</sup>A reader affects plant growth and fruit shape. *Plant Sci.* **2022**, *323*, 111417. [[CrossRef](#)] [[PubMed](#)]
23. Ao, Q.; Qiu, T.; Liao, F.; Hu, Z.; Yang, Y. Knockout of SIYTH2, encoding a YTH domain-containing protein, caused plant dwarfing, delayed fruit internal ripening, and increased seed abortion rate in tomato. *Plant Sci.* **2023**, *335*, 111807. [[CrossRef](#)] [[PubMed](#)]
24. Chen, C.; Wu, Y.; Li, J.; Wang, X.; Zeng, Z.; Xu, J.; Liu, Y.; Feng, J.; Chen, H.; He, Y.; et al. TBtools-II: A “one for all, all for one” bioinformatics platform for biological big-data mining. *Mol. Plant* **2023**, *16*, 1733–1742. [[CrossRef](#)] [[PubMed](#)]
25. Wilkins, M.R.; Gasteiger, E.; Bairoch, A.; Sanchez, J.C.; Williams, K.L.; Appel, R.D.; Hochstrasser, D.F. Protein identification and analysis tools in the ExPASy server. *Methods Mol. Biol.* **1999**, *112*, 531–552.
26. Marchler-Bauer, A.; Bo, Y.; Han, L.; He, J.; Lanczycki, C.J.; Lu, S.; Chitsaz, F.; Derbyshire, M.K.; Geer, R.C.; Gonzales, N.R.; et al. CDD/SPARCLE: Functional classification of proteins via subfamily domain architectures. *Nucleic Acids Res.* **2017**, *45*, D200–D203. [[CrossRef](#)] [[PubMed](#)]
27. Bailey, T.L.; Boden, M.; Buske, F.A.; Frith, M.; Grant, C.E.; Clementi, L.; Ren, J.; Li, W.W.; Noble, W.S. MEME SUITE: Tools for motif discovery and searching. *Nucleic Acids Res.* **2009**, *37*, W202–W208. [[CrossRef](#)] [[PubMed](#)]
28. Lescot, M.; Déhais, P.; Thijs, G.; Marchal, K.; Moreau, Y.; Van de Peer, Y.; Rouzé, P.; Rombauts, S. PlantCARE, a database of plant cis-acting regulatory elements and a portal to tools for in silico analysis of promoter sequences. *Nucleic Acids Res.* **2002**, *30*, 325–327. [[CrossRef](#)] [[PubMed](#)]
29. Zimmermann, P.; Hennig, L.; Grissem, W. Gene-expression analysis and network discovery using Genevestigator. *Trends Plant Sci.* **2005**, *10*, 407–409. [[CrossRef](#)]
30. Waese, J.; Provart, N.J. The Bio-Analytic Resource for Plant Biology. *Methods Mol. Biol.* **2017**, *1533*, 119–148.
31. Wang, N.; Guo, T.; Wang, P.; Sun, X.; Shao, Y.; Liang, B.; Jia, X.; Gong, X.; Ma, F. Functional analysis of apple *MhYTP1* and *MhYTP2* genes in leaf senescence and fruit ripening. *Sci. Hortic.* **2017**, *221*, 23–32. [[CrossRef](#)]
32. Guo, T.; Zhang, X.; Li, Y.; Liu, C.; Wang, N.; Jiang, Q.; Wu, J.; Ma, F.; Liu, C. Overexpression of *MdARD4* Accelerates Fruit Ripening and Increases Cold Hardiness in Tomato. *Int. J. Mol. Sci.* **2020**, *21*, 6182. [[CrossRef](#)] [[PubMed](#)]
33. Guo, T.; Wang, N.; Xue, Y.; Guan, Q.; van Nocker, S.; Liu, C.; Ma, F. Overexpression of the RNA binding protein *MhYTP1* in transgenic apple enhances drought tolerance and WUE by improving ABA level under drought condition. *Plant Sci.* **2019**, *280*, 397–407. [[CrossRef](#)] [[PubMed](#)]
34. Wang, P.; Yin, L.; Liang, D.; Li, C.; Ma, F.; Yue, Z. Delayed senescence of apple leaves by exogenous melatonin treatment: Toward regulating the ascorbate-glutathione cycle. *J. Pineal Res.* **2012**, *53*, 11–20. [[CrossRef](#)] [[PubMed](#)]
35. Tian, F.; Yang, D.C.; Meng, Y.Q.; Jin, J.; Gao, G. PlantRegMap: Charting functional regulatory maps in plants. *Nucleic Acids Res.* **2020**, *48*, D1104–D1113. [[CrossRef](#)] [[PubMed](#)]
36. Szklarczyk, D.; Kirsch, R.; Koutrouli, M.; Nastou, K.; Mehryary, F.; Hachilif, R.; Gable, A.L.; Fang, T.; Doncheva, N.T.; Pyysalo, S.; et al. The STRING database in 2023: Protein-protein association networks and functional enrichment analyses for any sequenced genome of interest. *Nucleic Acids Res.* **2023**, *51*, D638–D646. [[CrossRef](#)] [[PubMed](#)]
37. Yin, S.; Ao, Q.; Tan, C.; Yang, Y. Genome-wide identification and characterization of YTH domain-containing genes, encoding the m<sup>6</sup>A readers, and their expression in tomato. *Plant Cell Rep.* **2021**, *40*, 1229–1245. [[CrossRef](#)] [[PubMed](#)]
38. Wang, N.; Yue, Z.; Liang, D.; Ma, F. Genome-wide identification of members in the YTH domain-containing RNA-binding protein family in apple and expression analysis of their responsiveness to senescence and abiotic stresses. *Gene* **2014**, *538*, 292–305. [[CrossRef](#)]
39. Fan, S.; Xu, X.; Chen, J.; Yin, Y.; Zhao, Y. Genome-wide identification, characterization, and expression analysis of m<sup>6</sup>A readers-YTH domain-containing genes in alfalfa. *BMC Genom.* **2024**, *25*, 18. [[CrossRef](#)]
40. Scutenaire, J.; Deragon, J.-M.; Jean, V.; Benhamed, M.; Raynaud, C.; Favory, J.-J.; Merret, R.; Bousquet-Antonelli, C. The YTH domain protein ECT2 is an m<sup>6</sup>A reader required for normal trichome branching in Arabidopsis. *Plant Cell* **2018**, *30*, 986–1005. [[CrossRef](#)]
41. Zhu, D.Z.; Zhao, X.F.; Liu, C.Z.; Ma, F.F.; Wang, F.; Gao, X.-Q.; Zhang, X.S. Interaction between RNA helicase ROOT INITIATION DEFECTIVE 1 and GAMETOPHYTIC FACTOR 1 is involved in female gametophyte development in Arabidopsis. *J. Exp. Bot.* **2016**, *67*, 5757–5768. [[CrossRef](#)] [[PubMed](#)]

42. Tanabe, A.; Tanikawa, K.; Tsunetomi, M.; Takai, K.; Ikeda, H.; Konno, J.; Torigoe, T.; Maeda, H.; Kutomi, G.; Okita, K.; et al. RNA helicase *YTHDC2* promotes cancer metastasis via the enhancement of the efficiency by which HIF-1 $\alpha$  mRNA is translated. *Cancer Lett.* **2016**, *376*, 34–42. [[CrossRef](#)] [[PubMed](#)]
43. Song, P.; Yang, J.; Wang, C.; Lu, Q.; Shi, L.; Tayier, S.; Jia, G. Arabidopsis *N*<sup>6</sup>-methyladenosine reader CPSF30-L recognizes FUE signals to control polyadenylation site choice in liquid-like nuclear bodies. *Mol. Plant* **2021**, *14*, 571–587. [[CrossRef](#)] [[PubMed](#)]
44. Ouyang, Z.; Duan, H.; Mi, L.; Hu, W.; Chen, J.; Li, X.; Zhong, B. Genome-wide identification and expression analysis of the YTH domain-containing RNA binding protein family in *Citrus sinensis*. *J. Am. Soc. Hort. Sci.* **2019**, *144*, 79–91. [[CrossRef](#)]
45. Patil, D.P.; Pickering, B.F.; Jaffrey, S.R. Reading m<sup>6</sup>A in the Transcriptome: m<sup>6</sup>A-Binding Proteins. *Trends Cell Biol.* **2018**, *28*, 113–127. [[CrossRef](#)] [[PubMed](#)]
46. Arribas-Hernández, L.; Simonini, S.; Hansen, M.H.; Paredes, E.B.; Bressendorff, S.; Dong, Y.; Østergaard, L.; Brodersen, P. Recurrent requirement for the m<sup>6</sup>A-ECT2/ECT3/ECT4 axis in the control of cell proliferation during plant organogenesis. *Development* **2020**, *147*, dev189134. [[CrossRef](#)] [[PubMed](#)]
47. Vicente, A.M.; Manavski, N.; Rohn, P.T.; Schmid, L.M.; Garcia-Molina, A.; Leister, D.; Seydel, C.; Bellin, L.; Möhlmann, T.; Ammann, G.; et al. The plant cytosolic m<sup>6</sup>A RNA methylome stabilizes photosynthesis in the cold. *Plant Commun.* **2023**, *4*, 100634. [[CrossRef](#)]
48. Wang, S.; Wang, H.; Xu, Z.; Jiang, S.; Shi, Y.; Xie, H.; Wang, S.; Hua, J.; Wu, Y. m<sup>6</sup>A mRNA modification promotes chilling tolerance and modulates gene translation efficiency in Arabidopsis. *Plant Physiol.* **2023**, *192*, 1466–1482. [[CrossRef](#)]
49. Wang, N.; Guo, T.; Sun, X.; Jia, X.; Wang, P.; Shao, Y.; Liang, B.; Gong, X.; Ma, F. Functions of two *Malus hupehensis* (Pamp.) Rehd. YTPs (*MhYTP1* and *MhYTP2*) in biotic- and abiotic-stress responses. *Plant Sci.* **2017**, *261*, 18–27. [[CrossRef](#)]
50. Shen, L. Functional interdependence of *N*<sup>6</sup>-methyladenosine methyltransferase complex subunits in Arabidopsis. *Plant Cell* **2023**, *35*, 1901–1916. [[CrossRef](#)]
51. Sarowar, S.; Oh, H.W.; Cho, H.S.; Baek, K.H.; Seong, E.S.; Joung, Y.H.; Choi, G.J.; Lee, S.; Choi, D. Capsicum annum CCR4-associated factor CaCAF1 is necessary for plant development and defence response. *Plant J.* **2007**, *51*, 792–802. [[CrossRef](#)] [[PubMed](#)]
52. Liang, W.; Li, C.; Liu, F.; Jiang, H.; Li, S.; Sun, J.; Wu, X.; Li, C. The Arabidopsis homologs of CCR4-associated factor 1 show mRNA deadenylation activity and play a role in plant defence responses. *Cell Res.* **2009**, *19*, 307–316. [[CrossRef](#)] [[PubMed](#)]
53. Zhou, H.R.; Lin, R.N.; Huang, H.W.; Li, L.; Cai, T.; Zhu, J.K.; Chen, S.; He, X.J. The CCR4-NOT complex component NOT1 regulates RNA-directed DNA methylation and transcriptional silencing by facilitating Pol IV-dependent siRNA production. *Plant J.* **2020**, *103*, 1503–1515. [[CrossRef](#)] [[PubMed](#)]
54. Pereira, P.A.; Boavida, L.C.; Santos, M.R.; Becker, J.D. AtNOT1 is required for gametophyte development in Arabidopsis. *Plant J.* **2020**, *103*, 1289–1303. [[CrossRef](#)]
55. Motomura, K.; Arae, T.; Araki-Uramoto, H.; Suzuki, Y.; Takeuchi, H.; Suzuki, T.; Ichihashi, Y.; Shibata, A.; Shirasu, K.; Takeda, A.; et al. AtNOT1 Is a Novel Regulator of Gene Expression during Pollen Development. *Plant Cell Physiol.* **2020**, *61*, 712–721. [[CrossRef](#)]

**Disclaimer/Publisher’s Note:** The statements, opinions and data contained in all publications are solely those of the individual author(s) and contributor(s) and not of MDPI and/or the editor(s). MDPI and/or the editor(s) disclaim responsibility for any injury to people or property resulting from any ideas, methods, instructions or products referred to in the content.